11 A Goodwin-type Model with Cubic Investment Function

Iryna Sushko, Tönu Puu and Laura Gardini

11.1 Introduction

The present chapter is in the Goodwin (1951) tradition, with all bounds incorporated in the investment function, even the ceiling, which means that it is the investors who abstain from investing more once available resources put a limit on further expansion (in real terms). Goodwin modelled a continuous-time process, as described in Chapter 10, whereas the present model is cast in discrete time.

Goodwin further advocated a smooth investment function with asymptotes, such as a hyperbolic tangent shape. One of the present authors, Puu (1989) suggested a combination of linear-cubic terms in the investment function. The back-bending, caused by the cubic, needed to be given a factual explanation in terms of economics. Even if the complete model could be tuned so as to limit motion so that the cubic never hit the axes, which would be absurd, the existence of a maximum and a minimum were still responsible for some of the more exotic phenomena, and so needed an explanation.

This was not difficult. If one considers the hyperbolic tangent shape of the investment function as relevant for private investments, one could in addition consider public investments. In particular long-term budgets for infrastructure investments tend to be countercyclically distributed. This is partly due to an active wish to fight excessive changes in the cycle causing unemployment or inflation, and partly due to the advantage of using idle resources and low costs in the slump rather than in the boom.

A slightly different model was studied in Puu and Sushko (2004). The setup was as follows: Consumption was defined as $C_t = (1-s)Y_{t-1} + \varepsilon s Y_{t-2}$, where $0 < s < 1$ was the complementary proportion saved (or, in terms of other chapters of this book, $1 - s = c$), and a fraction $0 < \varepsilon < 1$ of savings was assumed to be spent after being saved for one period. Investment was defined as $I_t = v((Y_{t-1} - Y_{t-2}) - (Y_{t-1} - Y_{t-2})^3)$. To this we add the income identity $Y_t = C_t + I_t$. As we see, the consumption and investment variables can be eliminated, and the model cast as a second order recurrence equation in income alone, though containing a cubic nonlinearity.

The setup of the model just described obviously is non-generic, as the investment function is symmetric with respect to the origin. The aim of the present study is to also include an even order quadratic term to the investment function: $I_t = a((Y_{t-1} - Y_{t-2}) + b(Y_{t-1} - Y_{t-2})^2 - (Y_{t-1} - Y_{t-2})^3)$, so as to break the symmetry, and produce a more generic model. The consumption function is defined as $C_t = cY_{t-1}$, thus skipping the two-period lagged setup of Puu and Sushko (2004). As before, substituting to the income identity, we get a second order difference equation in income variable:

$$Y_t = cY_{t-1} + a((Y_{t-1} - Y_{t-2}) + b(Y_{t-1} - Y_{t-2})^2 - (Y_{t-1} - Y_{t-2})^3). \quad (1)$$

11.2 Description of the Map

Let $x_t := Y_t$, $y_t := Y_{t-1}$. Then to describe the dynamics of the model introduced above we have to study the behavior of trajectories of a two-dimensional map $F : \mathbb{R}^2 \to \mathbb{R}^2$ given by

$$F : \begin{pmatrix} x \\ y \end{pmatrix} \mapsto \begin{pmatrix} cx + a(x-y) + ab(x-y)^2 - a(x-y)^3 \\ x \end{pmatrix}, \qquad (2)$$

where a, b and c are real parameters such that

$$a > 0,\ 0 < c < 1. \qquad (3)$$

The parameter b is responsible for the symmetry of the investment function, namely, for $b = 0$ the 'floor' and 'ceiling' are located at equal distance from the origin, while the case $b \neq 0$ is more general.

In this chapter we shall illustrate some local and global bifurcation mechanisms related to the Neimark-Sacker bifurcation in a smooth map (already introduced in Chapter 1). We shall see how the stability loss of the fixed point with a pair of complex-conjugate eigenvalues on the unit circle results in the appearance (in the neighborhood of the fixed point) of an attracting closed invariant curve homeomorphic to a circle[1], and how this curve can be destroyed leading to complex dynamics.

[1] In invertible maps it is also called a two-dimensional torus, being associated with the Poincaré section of a three dimensional flow.

To begin, let us derive some simple properties of the map F. First note that F is a *noninvertible* map: In the phase space there exist two straight lines denoted LC_{-1} and LC'_{-1}, which are related to the vanishing determinant of the Jacobian matrix of F:

$$\begin{aligned} LC_{-1} &= \{(x,y) : y = x - k_1\}\,, \\ LC'_{-1} &= \{(x,y) : y = x - k_2\}\,, \end{aligned}$$

where $k_1 = (b - \sqrt{b^2+3})/3$, $k_2 = (b + \sqrt{b^2+3})/3$. Images of these lines by F are also straight lines, called *critical lines* and denoted LC and LC', respectively:

$$\begin{aligned} LC &= \left\{(x,y) : y = x/c - ak_1(k_1^2 - bk_1 - 1)\right\}\,, \\ LC' &= \left\{(x,y) : y = x/c - ak_2(k_2^2 - bk_2 - 1)\right\}\,. \end{aligned}$$

The role of the critical curves LC and LC' is related to the foliation of the Riemann phase plane: Any point between these two lines has three different preimages, while any point outside this strip has only one preimage. Thus, the map F has a noninvertibility of so-called $(Z_1 - Z_3 - Z_1)$ type. Other examples of maps with such a kind of noninvertibility can be seen in Mira *et al*. (1996), Dieci *et al*. (2001), Chiarella *et al*. (2002), Puu and Sushko (2004), Bischi *et al*. (2005).

It is known that the critical lines and their images play an important role for the dynamics of a noninvertible map (for a survey see Mira *et al*. (1996)). As we shall see, these images may define the boundary of an absorbing area to which the attractors of the map, as well as other invariant sets, necessarily belong. A contact of the boundary of some basin of attraction with the critical lines usually results in a global bifurcation causing the appearance of new isolated islands of the basin (Mira *et al*. (1994)). Regarding to an invariant attracting closed curve, which is the main interest of the present chapter, we shall see that the intersection of this curve with LC_{-1} or LC'_{-1} can give rise to the appearance of infinitely many loops, which are impossible in invertible maps (as already emphasized in Mira *et al*. (1996), Frouzakis *et al*. (1997)). We shall also see other features of closed invariant curves, related, in particular, to the homoclinic bifurcation, described in Chapter 1 and Chapter 8 for a fixed point, while here it will be related to a cycle of period 7.

Let us first describe the simplest kind of attractor of the map F, that is, its fixed point. It can be easily seen that F has a unique fixed point

$(x^*, y^*) = (0, 0)$. The eigenvalues of the Jacobian matrix of F at (x^*, y^*) depend on the parameters a and c:

$$\lambda_{1,2} = (a + c \pm \sqrt{(a + c)^2 - 4a})/2, \tag{4}$$

from which we deduce that for the parameter range given in (3) the fixed point (x^*, y^*) is a node if $(c+a)^2 > 4a$, and a focus if $(c+a)^2 < 4a$, being attracting for $a < 1$ and repelling for $a > 1$.

So, for $a < 1$ the fixed point of F is attracting, but it obviously cannot be a global attractor: Due to the cubic shape of the function defining our map, there are initial points whose trajectories are divergent. Indeed, the basin of attraction of the fixed point is bounded by the closure of the stable manifold of a saddle cycle of period 2, denoted $\{p_1, p_2\}$, where $p_1(x_0, y_0) = (bk/(1 - c) + \sqrt{k/a}/2, bk/(1 - c) - \sqrt{k/a}/2)$, $k = (c + 2a + 1)/2$ and $p_2 = F(p_1)$.

It can be verified that for the parameter range here considered the saddle cycle $\{p_1, p_2\}$ always exists (as an example, see Fig.2), and its stable manifold separates the basin of divergent trajectories from the set of points of the phase plane having bounded trajectories (which may include several disjoint basins and invariant sets). Running ahead we can say that the contact of an attractor with the stable manifold of this saddle results in a *boundary crises* which causes an explosion of the basin of divergent trajectories. Often, after such a contact, almost all the trajectories of F go to infinity and the surviving set is a *chaotic repellor* with a Cantor like structure (although a surviving attractor may also exist, with a basin of attraction so small that it is numerically unobservable).

11.3 Neimark-Sacker Bifurcation and Arnol'd Tongues

At $a = 1$ the fixed point (x^*, y^*) has complex-conjugate eigenvalues on the unit circle. It is known that if there is no so-called *strong resonance,* that is $\mathrm{Re}\,\lambda_{1,2} \neq \cos 2\pi m/n$, where $n \leq 4$, and m/n is an irreducible fraction, then a Neimark-Sacker bifurcation occurs resulting, when supercritical, in an attracting invariant closed curve $\mathcal{C}$ homeomorphic to a circle, which appears in the neighborhood of the fixed point. Note that other generic transversality conditions have to be also fulfilled, see Guckenheimer and Holmes (1985), Kuznetsov (1998). It can be verified that these conditions are satisfied for the parameter range here considered.

The dynamics of the map F on the curve $\mathcal{C}$ are either periodic or quasiperiodic, depending on the parameters. Namely, if at $a = 1$ also the condition

$$c = c_{m/n} \stackrel{def}{=} 2\cos(2\pi m/n) - 1, \tag{5}$$

holds, then after the bifurcation, that is for $a = 1 + \varepsilon$ for a sufficiently small $\varepsilon > 0$, a pair of cycles of period n, an attracting node and a saddle, with rotation number m/n exist on the curve $\mathcal{C}$ (also called a phase-locked torus), so that this curve is made up by the closure of the unstable manifold of the saddle cycle. Note that for $c > 0$ we have $m/n < 1/6$. While if

$$c = c_\rho \stackrel{def}{=} 2\cos(2\pi\rho) - 1, \tag{6}$$

where ρ is an irrational number, then after the bifurcation there are quasiperiodic trajectories on the curve $\mathcal{C}$ (also called quasiperiodic torus).

The dynamics of F locally, in the neighborhood of the fixed point, depend only on the parameters a and c, while the parameter b influences, obviously, the global dynamics. Due to the symmetry with respect to the origin of the map F for negative and positive values of b, we can restrict our analysis only to the case $b > 0$ (the case $b < 0$ is analogous, with trajectories symmetric with respect to the origin in the phase space, and symmetric structure of the parameter space). We don't consider in this chapter the particular value $b = 0$, however in such a case F has dynamics qualitatively similar to those described in Puu and Sushko (2004).

Fig.1 presents a two-dimensional bifurcation diagram of the map F in the (a, c)-parameter plane at $b = 0.2$, where the parameter regions corresponding to the attracting cycles of different periods $n \leq 32$, are shown by different gray tonalities. The periodicity regions starting from the bifurcation line $a = 1$ are called *Arnol'd tongues*. It is known that the boundaries of the Arnol'd tongue are two curves corresponding to saddle-node bifurcation of the related cycles (the lower and upper boundaries of the periodicity tongues in Fig.1), while other boundaries (to the right) are related to either period-doubling or Neimark-Sacker bifurcation of the related attracting cycle. The periodicity tongue associated with the rotation number m/n starts from the parameter point $(a, c) = (1, c_{m/n})$, while the parameter point $(a, c) = (1, c_\rho)$ is the starting point for the curve corresponding to a closed curve with quasiperiodic trajectories, related to the irrational rotation number ρ. Such a structure of the parameter plane reflects the Neimark-Sacker bifurcation theorem mentioned above, according to which for the parameter values taken near the bifurcation line $a = 1$, that is for $a = 1 + \varepsilon$ for some sufficiently small $\varepsilon > 0$, in the neighborhood of the fixed point there exists an attracting invariant closed curve $\mathcal{C}$ on which the map F is reduced to a rotation with rational or irrational rotation number. Examples of the curve $\mathcal{C}$ in case of rotation numbers $1/6$ and $1/7$ can be seen in Fig.2 and Fig.8, respectively.

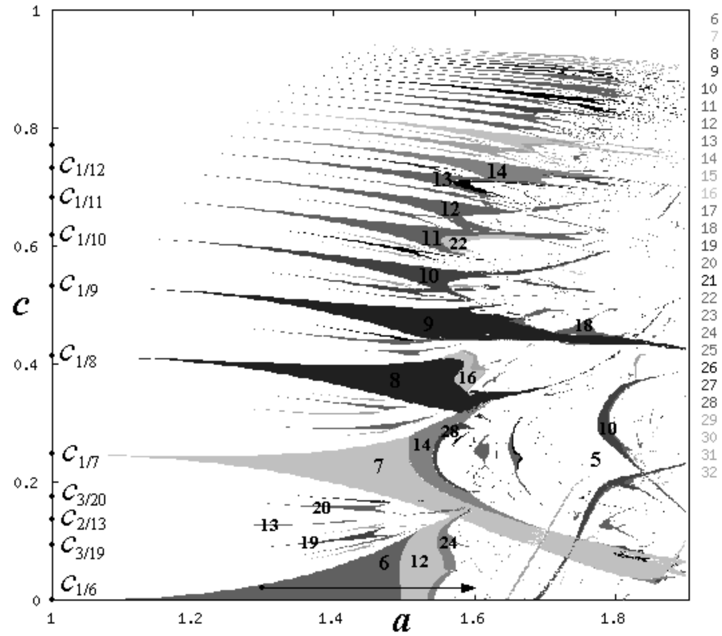

Figure 1: *Two-dimensional bifurcation diagram of the map* F *in the* (a, c)*-parameter plane for* $b = 0.2$*. Parameter regions related to attracting cycles of different periods* $n \leq 32$ *are shown by different gray tonalities.*

At fixed value of c, on increasing the value of a the curve $\mathcal{C}$ is destroyed and the dynamics of F become more complicated. Let us first recall in short possible scenarios leading to the destruction of a closed invariant attracting curve:

(1) The related attracting cycle, being a node at its birth, becomes a focus. We can say that the closed invariant curve still exists but it is no longer homeomorphic to a circle (an example can be seen in Fig.8). In such a case it is quite common that when the parameter point leaves the periodicity tongue

then the attracting focus undergoes a Neimark-Sacker bifurcation, and cyclical closed invariant curves appear;

(2) The related attracting cycle can undergo period-doubling bifurcation;

(3) The curve $\mathcal{C}$ can lose its smoothness and becomes nondifferentiable (due to infinitely many oscillations of one branch of the unstable manifold of the saddle, approaching the node);

(4) The related saddle cycle undergoes homoclinic bifurcation;

(5) Intersection of the curve $\mathcal{C}$ with a critical line can lead to the creation of infinitely many loops, that is, to the selfintersections of the unstable manifold of the saddle (see Fig.3).

If the parameter point leaves the periodicity tongue crossing the saddle-node bifurcation curve when $\mathcal{C}$ is still smooth, then we have transition from the phase-locked torus to the quasiperiodic one. In the two cases (3) and (4), if the parameter point leaves the periodicity tongue crossing the saddle-node bifurcation curve, then the curve $\mathcal{C}$ is transformed into a set with fractal structure.

The destruction of a two-dimensional torus in the case of diffeomorphisms was first described in Afraimovich and Shil'nikov (1983). In Aronson *et. al*. (1982) it was in particular shown that torus can be destroyed also due to the contact with its basin boundary. See also Anishchenko *et al*. (1994), Arnol'd *et al*. (1991) for further details and examples. The first four scenarios can occur both in invertible and noninvertible maps (for the examples related to noninvertible maps see Gumowski and Mira, (1980a,b)), while the case (5) obviously can occur only for a noninvertible map (several examples are given in Mira *et al*. (1996), Frouzakis *et al*. (1997), Maistrenko *et al.* (2003)), and one example will be given also in the next section.

In the last section we shall describe a sequence of transformations occurring at fixed c and increasing a, associated with a 7-node, which becomes at first a 7-focus (i.e. case (1) above), then it becomes a 7-node again (with one negative eigenvalue), which undergoes the flip bifurcation. Futher increase of a leads to appearance of two 7-cyclical closed invariant curves, attracting and repelling, via global bifurcations as described in Chapters 1 and 8.

To close this section we mention an important feature of nonlinear maps for parameter values taken far from the Neimark-Sacker bifurcation curve, which is that the periodicity regions can be overlapped (as it can be seen in Fig.1 or Fig.7). This means that coexistence of attracting cycles of different periods is not a rare phenomenon, and usually this situation leads to several kinds of global bifurcations in the invariant sets and/or in the basins of attraction of the coexisting attracting sets.

11.4 First example of bifurcation sequence: Creation of loops and period-doubling cascade

In this section we present a bifurcation scenario of transition to complex dynamics, related to the destruction of the closed invariant curve $\mathcal{C}$ via creation of infinitely many loops (an effect of the noninvertibility, leading to the self-intersections of the unstable set of the saddle cycle), and the period-doubling cascade of the attracting cycle existing on $\mathcal{C}$.

Let γ_n denote an attracting cycle of period n, and γ_n^+, γ_n^-, denote saddle cycles of period n with, respectively, positive and negative eigenvalue related to the unstable eigendirection.

For the first example we fix $b = 0.2$ and $c = 0.02$ and will increase a starting from $a = 1.3$, as shown in Fig.1 by the straight line with an arrow. The phase portrait of the map F at $a = 1.3$ is presented in Fig.2: There exists an attracting invariant closed curve $\mathcal{C}$ made up the unstable manifold of the saddle cycle γ_6^+ approaching points of the attracting cycle γ_6. The

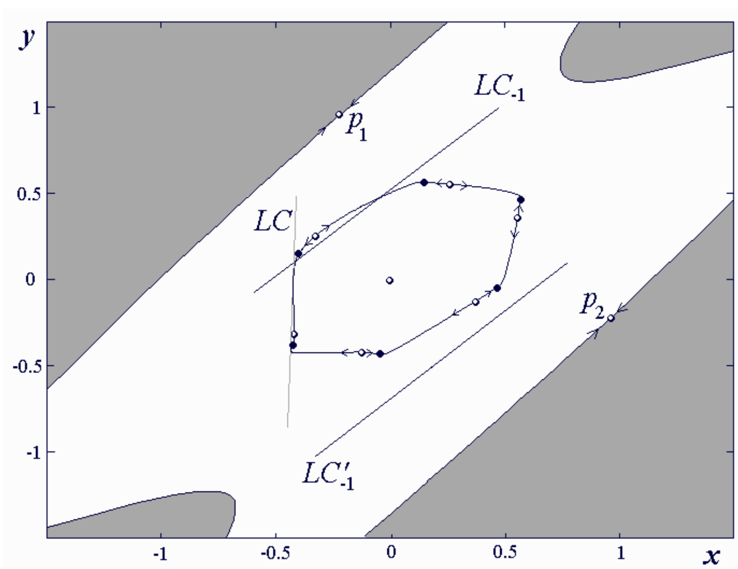

Figure 2: *Phase portrait of the map F at $a = 1.3$, $b = 0.2$, $c = 0.02$. The attracting closed invariant curve is formed by the closure of the unstable manifold of the saddle 6-cycle (shown by white circles), approaching the points of the attracting 6-cycle (the black circles).*

basins of attraction of $\mathcal{C}$ and that of infinity (i.e., of divergent trajectories) are separated by the stable manifold of the saddle cycle $\{p_1, p_2\}$. It can be seen that the curve $\mathcal{C}$ intersects the critical line LC_{-1} and is folded on LC (i.e., tangent to LC and bent to the right) without creation of loops, which in particular means that the map F is invertible on $\mathcal{C}$, and $\mathcal{C}$ is homeomorphic to a circle. However, it is worth noticing that the area bounded by $\mathcal{C}$ is not invariant under application of F: In fact it is invariant only as long as the closed curve $\mathcal{C}$ has no intersections with the lines LC_{-1} and LC'_{-1}, and this is no longer true in the case shown in Fig.2. According to the results stated in Frouzakis *et al.* (1997) (see also Maistrenko *et al.* (2003)), the cusp points and then the loops are created on $\mathcal{C}$ if the slope of the tangent of the curve $\mathcal{C}$ at the point of intersection with LC_{-1} (or LC'_{-1}) at first is the same and then becomes larger then the slope of the eigenvector associated with the zero eigenvalue of the Jacobian matrix of the map F at that point. Fig.3 shows the curve $\mathcal{C}$ at $a = 1.45$ when the loops are already created, thus the map F is noninvertible on the curve $\mathcal{C}$, which obviously is no longer homeomorphic to a circle.

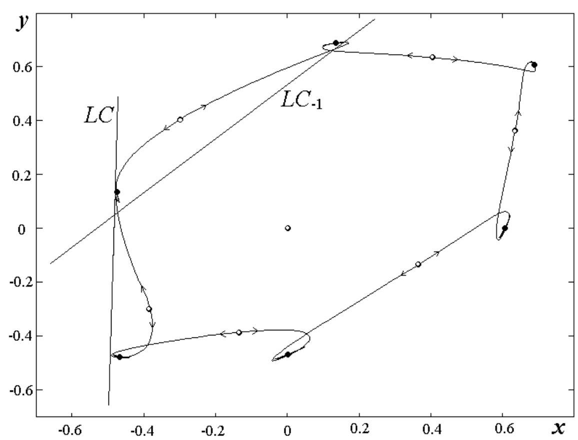

Figure 3: *The attracting closed invariant curve* $\mathcal{C}$ *with infinitely many loops at* $a = 1.45$, $b = 0.2$, $c = 0.02$.

If we continue to increase the values of a, the cycle γ_6 undergoes a cascade of the period-doubling bifurcations: At $a \approx 1.4952$ the first period-doubling bifurcation occurs resulting in a saddle γ_6^- and attracting cycle γ_{12}. Fig.4 presents the phase portrait of the map F at $a = 1.5$, where the attracting cycle γ_{12} and two saddle cycles γ_6^+ and γ_6^- are shown, together with the unstable manifold of γ_6^+, which has infinitely many loops. The value $a = a^* \approx 1.548481$ is a limit for the values related to the period-doubling cascade of the cycle γ_6. Approaching the value a^* from the opposite side we have a cascade of homoclinic bifurcations for the saddle cycles γ_{6k}^-, $k = 1, ...$, born during the period-doubling cascade of γ_6. Each of these homoclinic bifurcations gives rise to the pairwise merging of pieces of cyclic chaotic attractors. As an example, Fig.5 shows the 12-piece chaotic attractor at $a = 1.56$, near the first homoclinic bifurcation of the cycle γ_6^- (shown by the gray circles). The result of this homoclinic bifurcation is a 6-piece chaotic attractor.

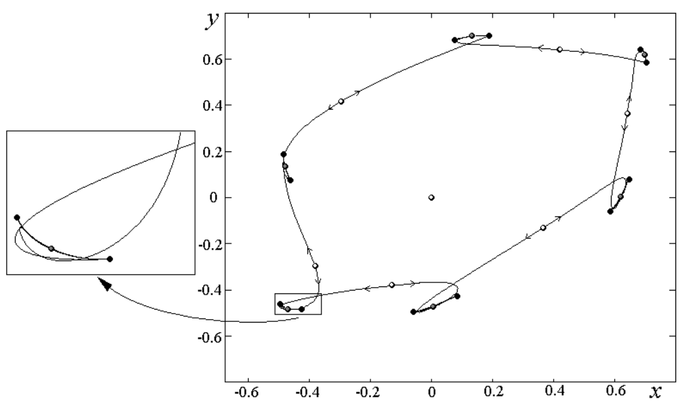

Figure 4: *The phase portrait of the map F and its enlarged part at $a = 1.5$, $b = 0.2$, $c = 0.02$: The points of the saddle cycles γ_6^+ and γ_6^-, are shown by white and gray circles, respectively; Black circles indicate points of the attracting cycle γ_{12}.*

The basin of attraction of each of the 6 pieces of the chaotic attractor is separated by the stable manifold of the saddle cycle of period 6, while the unstable branches tend to the attractor (indeed, the closure of the unstable set of the saddle includes the chaotic pieces). Thus, if we consider the map F^6, a contact of the chaotic pieces with the boundary of their immediate basins results in the first homoclinic bifurcation of the 6-saddle. Such a bifurcation gives rise to the merging of these 6 pieces into a one piece chaotic attractor. Fig.6(a) presents a one-piece chaotic attractor soon after this contact bifurcation. In general such a transition is accompanied by a so-called “rare points” phenomenon, reflecting the difference in density of the points along the attractor, as explained in detail in Mira *et al*. (1996), Gardini *et al*. (1996), Maistrenko *et al*. (1998).

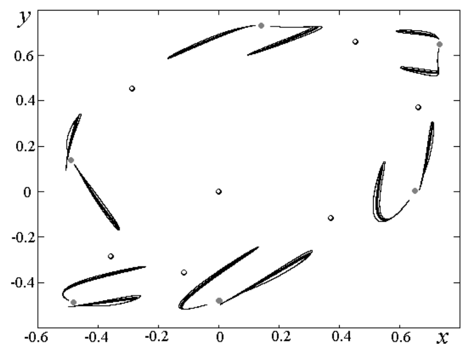

Figure 5: *The* 12*-piece cyclic chaotic attractor of the map* F *at* $a = 1.56$, $b = 0.2$, $c = 0.02$.

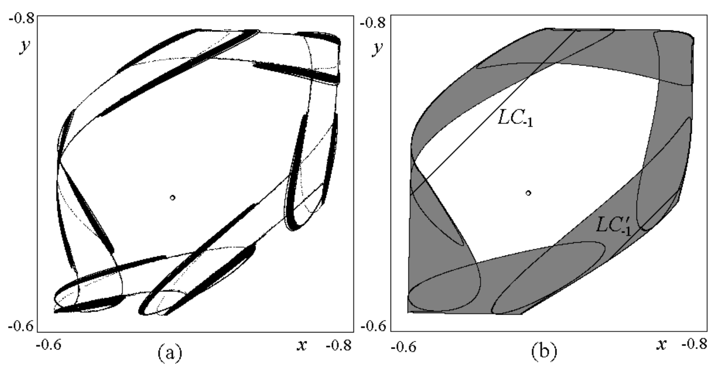

Figure 6: *(a) One-piece chaotic attractor of the map* F *at* $a = 1.5802$, $b = 0.2$*,* $c = 0.02$; *(b) Its absorbing area.*

All the attracting sets of the map F existing in the considered parameter range, after the bifurcation of the fixed point (see Fig.2 up to Fig.6(a)) belong to an absorbing area which is obtained by taking the images of a few segments of LC_{-1} and LC'_{-1}, which are exactly those pieces inside the area. An example is shown in Fig.6(b): The area is bounded by six images of the indicated segments of LC_{-1} and LC'_{-1}. The simply connected area is invariant, while the annular area, shown in gray in Fig.6(b), which more strictly includes all the existing invariant sets (except for the repelling fixed point), is absorbing but not invariant: A thinner annular invariant area can be obtained by using further images of the critical segments.

11.5 Second example: focus, bistability and global bifurcations of closed invariant curves

In this section we present one more example of bifurcation sequence which includes the destruction of the closed invariant curve $\mathcal{C}$ followed by a particular type of global bifurcation. This transition to complex dynamics is more complicated with respect to the one described in the previous section, as it includes bistability and one more Neimark-Sacker bifurcation. A global bifurcation related to this "secondary" Neimark-Sacker bifurcation will be emphasized, which gives rise to a pair of cyclical closed invariant curves, one attracting and one repelling.

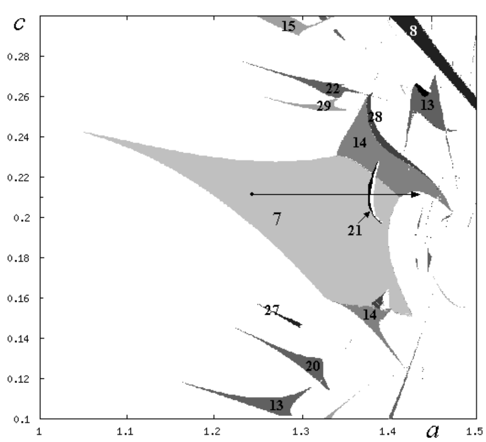

Figure 7: *Two-dimensional bifurcation diagram of the map F in the (a, c)-parameter plane at $b = 0.5$.*

We present a sequence of bifurcations related to the attracting cycle γ_7, fixing the parameters $b = 0.5$, $c = 0.21$ and increasing the value a starting from $a = 1.24$. The corresponding parameter path is shown in Fig.7 by the straight line with an arrow. The phase portrait of the map F at $a = 1.24$ is qualitatively similar to the one shown in Fig.2: Namely, there exists a closed attracting invariant curve $\mathcal{C}$, homeomorphic to a circle, made up by the unstable manifold of the saddle cycle γ_7^+, approaching the points of the attracting node γ_7. Increasing a the cycle γ_7 becomes a focus (see Fig.8 where $a = 1.31$), so that the curve $\mathcal{C}$ is no longer homeomorphic to a circle. The basins of attraction of each point of the attracting cycle γ_7 (considering

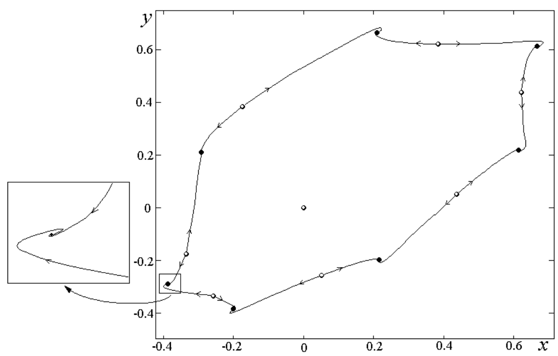

Figure 8: *The phase portrait and its enlarged part of the map F at $a = 1.31$, $b = 0.5$, $c = 0.21$.*

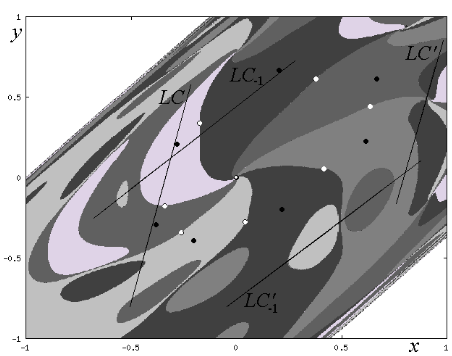

Figure 9: *Individual basins of attraction of points of the attracting cycle γ_7 (the black circles), bounded by the stable manifold of the saddle cycle γ_7^+ (the white circles).*

the map F^7) is presented in Fig.9: The boundary, formed by the stable manifold of the saddle cycle γ_7^+ has a regular structure. The intersection of the basin with the critical lines LC and LC' creates disconnected components of the basins, located on LC_{-1} and LC'_{-1}.

Increasing a a saddle-node bifurcation occurs giving rise to an attracting and a saddle cycle of period 21, and, thus, to bistability: Fig.10 presents the phase portrait of the map F at $a = 1.378$, with the attracting cycles γ_7 and γ_{21} (shown by big and small black circles, respectively), the saddle cycle γ_{21}^+ (the black squares) and the repelling cycle of period 7 (the white circles), which is the former saddle cycle γ_7^+ after the period-doubling bifurcation resulted in the saddle cycle γ_{14}^+ (white squares). The basin of attraction of the cycle γ_{21} is shown in white, while the basin of attraction of γ_7 is shown in dark gray. These two basins are separated by the stable set of γ_{21}^+. The light gray region corresponds to divergent trajectories. Further development of

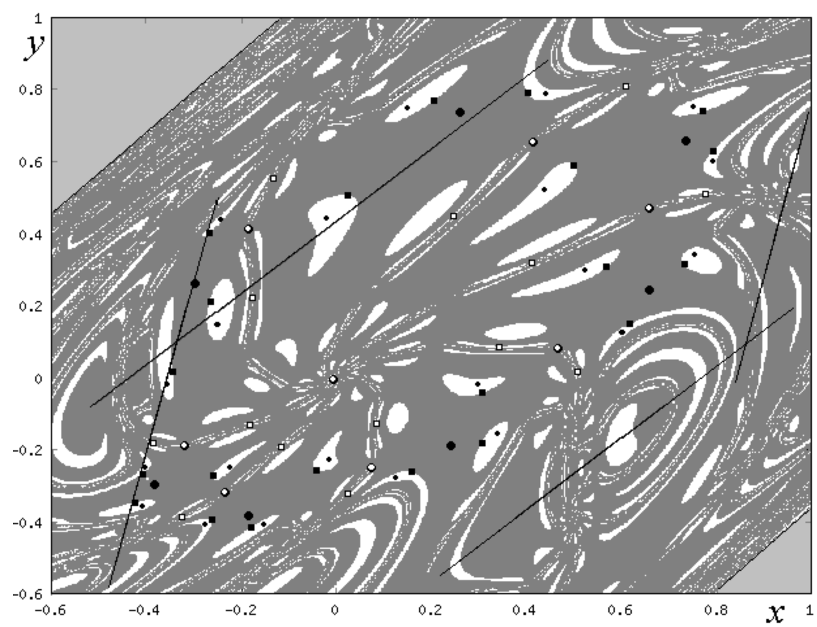

Figure 10: *The phase portrait of the map F at $a = 1.378$, $b = 0.5$, $c = 0.21$ with coexisting attracting cycles γ_{21} and γ_7 whose basins of attraction are shown in white and gray, respectively.*

the scenarios, increasing a, is related to the cascade of the period-doubling bifurcations of the cycle γ_{21}. Fig.11 shows an enlarged part of the phase space with several pieces of a 21-piece cyclic chaotic attractor coexisting with the attracting cycle γ_7 at $a = 1.381$. This chaotic attractor disappears due to a boundary crises, i.e., a contact with its basin boundary, which at the same time is the first homoclinic bifurcation of the saddle cycle γ_{21}^{+}. Soon after this contact there is only one attractor, the cycle γ_7, surrounded by a chaotic repellor created at the mentioned homoclinic bifurcation.

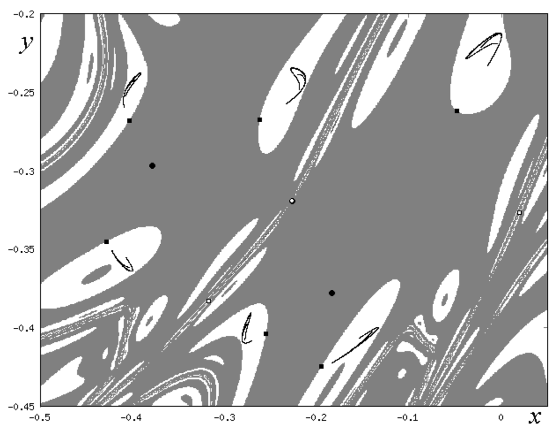

Figure 11: *An enlarged part of the phase space of the map* F *at* $a = 1.381$, $b = 0.5$, $c = 0.21$.

The parameter path shown in Fig.7 is chosen in such a way that at the exit of the 7-periodicity tongue the cycle γ_7 undergoes a period-doubling bifurcation resulting in a saddle cycle γ_7^- and an attracting cycle γ_{14}. For example, at $a = 1.41335$ the parameter point is inside the periodicity region corresponding to an attracting cycle γ_{14}. However, as a increases, the parameter point moves towards a region which is also close to the Neimark-Sacker bifurcation of the 7-cycle, and the global bifurcation may occur, already described in Chapters 1 and 8 (related there with a fixed point of the map). Indeed, such a global bifurcation has been detected, which gives rise to the appearance of a pair of disjoint 7-cyclical closed invariant curves, one attracting, denoted Γ_7, and one repelling, denoted Γ_7', surrounding the points of the saddle cycle γ_7^- and the attracting cycle γ_{14}. After the first homoclinic bifurcation of the cycle γ_7^- the curve Γ_7' undergoes pairwise splitting and becomes a 14-cyclical repelling closed invariant curve Γ'_{14}: The phase portrait of the map F at $a = 1.4134$ is shown in Fig.12 (a) and an enlargement is given in Fig.12 (b), where it can be seen one curve of Γ_7 and two curves of Γ'_{14}, which surround the points of the cycles γ_{14} and γ_7^-, shown by black and white circles, respectively. The 14-cyclical repelling closed invariant curve Γ'_{14} bounds the basin of attraction of γ_{14}, while the wider basin (among the points having bounded trajectories) is that of points attracting to Γ_7. As expected, on further increasing of a the cycle γ_{14} becomes unstable via a subcritical Neimark-Sacker bifurcation, leaving the 7-cyclical closed curve Γ_7 as unique attracting set.

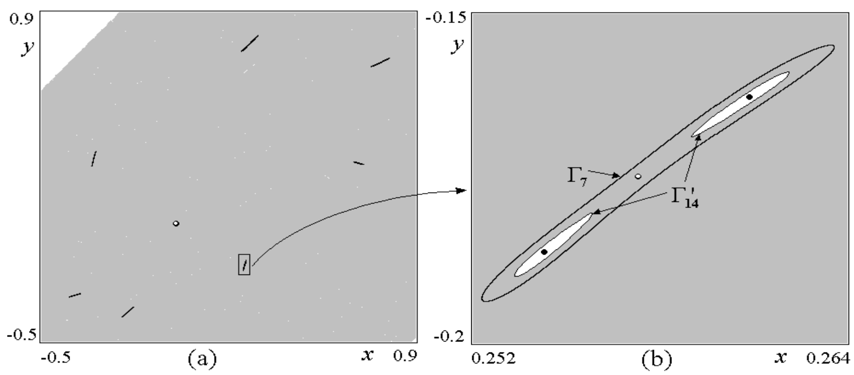

Figure 12: *In (a) the* 7*-cyclical attracting closed invariant curve* Γ_7 *is visible, while in the enlargement (b), besides one curve of* Γ_7*, it can be also seen two curves of the* 14*-cyclical repelling closed invariant curve* Γ'_{14}*, which bound the basin of attraction of the cycle* γ_{14}.

References

Afraimovich, V.S., Shil'nikov, L.P., 1983, "Invariant two-dimensional tori, their destruction and stochasticity", *Gorkii University*, Gorkii, Russia:3-26

Anishchenko, V.S, Safonova, M.A., Feudel, U., Kurths, J., 1994, "Bifurcations and transition to chaos through three-dimensional tori", *Int. J. Bif. and Chaos*, Vol. 4., No 3:595-607

Arnol'd, V.I., Afraimovich, V.S., Il'iashenko, Yu.S., Shil'nikov, L.P., 1991, *Dynamical Systems*, Vol. 5, Springer, Berlin

Aronson, D.G., Chory, M.A., Hall, G.R., McGehee, R.P., 1982, "Bifurcations from an invariant circle for two-parameter families of maps of the plane: A computer-assisted study", Commun. Math. Phys. 83:303-354

Bischi, G.I., Gardini, L., Mira, C., 2005, "Basin fractalization generated by a two-dimensional family of Z1-Z3-Z1 maps", *Int. J. Bif. and Chaos* (to appear)

Chiarella, C., Dieci, R., Gardini, L., 2002, "Speculative Behaviour and Complex Asset Price Dynamics: A Global Analysis", *Journal of Economic Behavior and Organization*, 49(1)

Dieci, R., Bischi, G.-I., Gardini L., 2001, "Multistability and role of noninvertibility in a discrete-time business cycle model", *Central European Journal of Operation Research*, Vol. 9:71-96

Frouzakis, C.E., Gardini, L., Kevrekidis, I.G., Millerioux, G., Mira, C., 1997, "On some properties of invariant sets of two-dimensional noninvertible maps", *Int. J. Bif. and Chaos*, Vol. 7, No. 6:1167-1194

Gandolfo, G., 1985, *Economic dynamics: methods and models*, Second edition, North Holland, Amsterdam

Gardini, L., Abraham, R., Record, R.J., Fournier-Prunaret, D., 1994, "A double logistic map", *Int. J. Bif. and Chaos*, 4:145-176

Gardini, L., Mira, C., Fournier-Prunaret, D., 1996, "Properties of invariant areas in two-dimensional endomorphisms", In book: *Iteration Theory*, W. Forg-Rob et al. ed.s, World Scientific:112-125

Goodwin, R.M., 1951, "The nonlinear accelerator and the persistence of business cycles", *Econometrica,* 19:1-17

Guckenheimer, J. and Holmes P., 1985, *Nonlinear Oscillations, Dynamical Systems, and Bifurcations of Vector Fields*, Springer-Verlag

Gumowski, I. and Mira, C., 1980a, *Dynamique chaotique*, Ed. Cépadues, Toulouse

Gumowski, I. and Mira, C., 1980b, *Recurrences and discrete dynamic systems*, Lecture notes in Mathematics, Springer

Herman, M., 1979, "Sur la cojugaison différentiable de difféomorphismes du cercle à des rotations", *Publ. Math.I.H.E.S.* 49:5-233

Hicks, J.R., 1950, *A contribution to the theory of the trade cycle*, Clarendon Press, Oxford

Kuznetsov, Yu., 1998, *Elements of Applied Bifurcation Theory*, Springer-Verlag, New York

Maistrenko, Y., Sushko, I., Gardini, L., 1998, "About two mechanisms of reunion of chaotic attractors", *Chaos, Solitons and Fractals,* Vol. 9, No. 8:1373-1390

Maistrenko, V., Maistrenko, Yu., Mosekilde, E., 2003, "Torus breakdown in noninvertible maps", *Physical Review E* 67, 046215

Mira, C., Fournier-Prunaret, D., Gardini, L., Kawakami, H., Cathala, J.C., 1994, "Basin bifurcations of two-dimensional noninvertible maps. Fractalization of basins", *Int. J. Bif. and Chaos*, 4(2):343-381

Mira, C., Gardini, L., Barugola, A., Cathala, J.C., 1996, *Chaotic Dynamics in Two-Dimensional Noninvertible Maps*, World Scientific, Singapore

Neimark, Y., 1959, "On some cases of periodic motions depending on parameters", *Dokl. Acad. Nauk SSSR* 129:736-739

Nitecki, Z., 1971, *Differentiable dynamics*, M.I.T. Press, Cambridge

Puu, T., 1989, *Nonlinear economic dynamics*, Lecture Notes in Economics and Mathematical Systems 336, Springer-Verlag, Berlin

Puu, T., Sushko, I., 2004, "A business cycle model with cubic nonlinearity", *Chaos, Solitons and Fractals*, 19:597-612

Sacker, R., 1965, "A new approach to the perturbation theory of invariant surfaces", *Comm. Pure Appl. Math*. 18:717-732